Phys. Status Solidi B **252,** No. 5, 1017–1023 (2015) / **DOI** 10.1002/pssb.201451579

physica status solidi b
www.pss-b.com
basic solid state physics

Mapping of inhomogeneity and thermal degradation of Au/Ni/n-GaN Schottky diodes using scanning internal photoemission microscopy

Shingo Yamamoto, Yuhei Kihara, and Kenji Shiojima*

Graduate School of Electrical and Electronics Engineering, University of Fukui, 3-9-1 Bunkyo, Fukui 910-8507, Japan

Received 30 September 2014, revised 12 December 2014, accepted 16 December 2014
Published online 27 January 2015

Keywords Schottky contacts, GaN, internal photoemission, gold, nickel

* Corresponding author: e-mail shiojima@u-fukui.ac.jp, Phone: +81776278560, Fax: +81776278749

We have developed a new mapping technique, termed scanning internal-photoemission microscopy, to characterize the electrical inhomogeneity of metal-semiconductor interfaces. We characterized the initial stage of thermal degradation of Au/Ni/n-GaN Schottky contacts. We found that, upon 400 °C annealing, a partial thermal degradation occurred from a scratch on the dot, where Au atoms diffused to the interface and reacted with GaN. When the top Au layer was partially missing, upon annealing, the Ni surface was oxidized and NiO_x/n-GaN with a small Schottky barrier height was formed. In addition, a thin contamination layer at the interface was clearly observed as a pattern. It was confirmed that this method is a powerful tool to map metal contacts for the investigations of partial thermal degradation, formation of parallel contacts, and inhomogeneity of surface chemistry.

1 Introduction Metal-to-semiconductor contacts are one of the most important elements in semiconductor device fabrication technologies. As an ohmic contact provides current injection between metal and semiconductors, a small contact resistance is required. As a Schottky contact provides rectifying characteristics, a small on-resistance, low reverse biased current, large breakdown voltage, and high speed operation are required. In the actual device fabrication, a large number of contacts are in one wafer, and the uniformity of the contacts should be guaranteed. In practical metal-to-semiconductor interfaces, there are some origins of inhomogeneity, such as crystal defects, process induced damages, surface contamination, interfacial reactions between metal and semiconductors, and so on.

As for conventional characterization of the contacts, current–voltage (I–V) and capacitance–voltage (C–V) methods are widely used. The averaged values of the contacts are obtained from these results. Recently, GaN-based materials have been the subject of intensive research for high-temperature/high-power electronic devices [1–3]. AlGaN/GaN high-electron-mobility-transistors (HEMT) have been successfully developed for the application of power amplifiers in base stations, and then the power switching application is of interest. As a result of commercialization of GaN free-standing substrates, vertical field-effect transistors [4], 1.1 kV Schottky diodes [5], and 3.0 kV p–n junction diodes [6] have been demonstrated. As the operation of such devices is in a higher temperature under a strong electrical field with a large current density, the device reliability is one of the most important issues for the commercialization. The actual device degradation mechanism has been reported with a formation of pits on the drain side of the gates in AlGaN/GaN HEMTs [7–9]. Two dimensional characterizations are useful to clarify the origin and mechanism of the device degradation.

For metal-to-semiconductor contacts, cross-sectional images of transmission electron microscopy (TEM) are very powerful in revealing metallurgical inhomogeneity, that is, interfacial phases, bonding structures [10], however, this method is destructive and the sample preparation requires mature skills. For mapping of electrical characteristics of the contacts, electron-beam induced current [11] and optical beam induced current techniques have been demonstrated, but, because the samples were irradiated through very thin

metal layers by means of electrons or monochromatic light, these methods are not available for the interface buried under a thick metal layer.

We have developed a new mapping technique termed scanning internal-photoemission microscopy (SIPM) to characterize the electrical inhomogeneity of metal–semiconductor interfaces. We demonstrated mapping of parallel Schottky contacts of Ni and Pd on n-Si [12], ion implantation damages in GaAs Schottky contacts [13], and thermal degradation of Au/Pt/Ti/n-GaAs Schottky contacts by using infrared lasers as a light source [14].

In this paper, we rebuild the SIPM measurement system to characterize widegap semiconductor contacts by using blue and green lasers. The mechanical precision was also improved. Au/Ni/n-GaN Schottky contacts were investigated with SIPM in addition to *I–V* and photoresponse (PR) methods, because Ni Schottky contacts are normally used for gate electrodes in AlGaN/GaN HEMTs and high-power Schottky diodes. In addition to conventional samples, metal dots with improper device fabrication processes were also prepared. The initial stage of thermal degradation of the contacts was investigated.

2 Sample preparation In this study, we used vertical high-voltage Schottky diodes as shown in Fig. 1. By using free-standing GaN substrates, the dislocation density was reduced to as low as $1 \times 10^6\,\mathrm{cm}^{-2}$. The donor concentration of the GaN substrate was $1 \times 10^{18}\,\mathrm{cm}^{-3}$. Two-μm-thick Si-doped n^+-GaN (Si:$2 \times 10^{18}\,\mathrm{cm}^{-3}$) and 11 μm thick n^--GaN (Si:$2 \times 10^{16}\,\mathrm{cm}^{-3}$) layers were grown as access and drift regions, respectively. Both layers were grown in a laminar flow MOCVD reactor using trimethylgallium and ammonia gas as precursors. The thickness and carrier concentration of the drift region were designed for a breakdown voltage of 1000 V. Firstly, the GaN surface was degreased in acetone and ethanol. Just after a surface treatment of HCl acid solution, Ti (20 nm)/Al (200 nm) was deposited on the rear surface by electron beam evaporation, and then rapid thermal annealing was conducted at 800 °C for 30 s. On the front surface, after an HCl surface treatment, Ni (50 nm)/Au (50 nm) Schottky contacts were deposited by the electron beam evaporation.

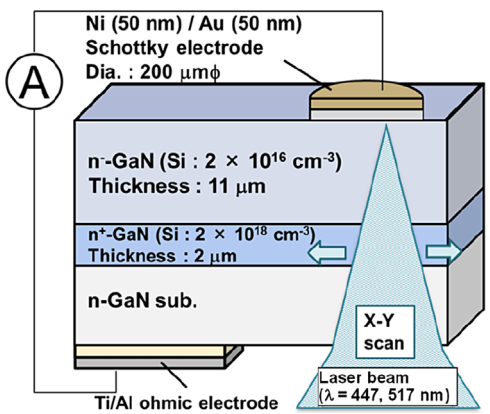

Figure 1 Sample structure.

We prepared four kinds of samples: (i) conventional dots as a control sample, (ii) scratched dots, in which the metal surface was scratched with small particles in wafer scribing and cleaving process, (iii) dots with partial removal of the only top Au layers, and (iv) dots processed in an improper surface treatment, where surface contamination patterns, so-called "water mark", were seen.

It has been reported that, the interfacial reaction between Ni and GaN occurred, and rectify characteristics were lost over 600 °C annealing [15, 16]. In this study, as we focused on the investigation of the initial stage of thermal degradation of the contacts, annealing was conducted at a relatively lower temperature of 400 °C for 10 min in Nitrogen ambient.

3 Measurement methods The *I–V* measurements were carried out by using an HP4142B semiconductor parameter analyser. The Schottky barrier height ($q\varphi_B$) was simply calculated in terms of the thermionic emission model [17] using

$$J = A^{**}T^2\exp(-q\varphi_B/kT)[\exp(qV/nkT) - 1], \qquad (1)$$

where A^{**} is the effective Richardson constant (26.4 $\mathrm{A/cm^2\,K^2}$ for n-GaN based on $A^{**} = 4\pi m^* q k^2/h^3$ and $m^* = 0.22m_0$), T is the temperature, q is the charge of the electron, k is the Boltzmann constant, and V is the applied voltage.

In the PR measurements, when a monochromatic light with a photon energy ($h\nu$) greater than $q\varphi_B$ is incident on a metal/GaN interface, carriers in the metal can surmount the Schottky barrier and a photocurrent may be generated, which is called the internal photoemission effect. The $q\varphi_B$ can be determined from the measured photocurrent, using Fowler's equation [18]

$$Y^{1/2} \propto (h\nu - q\varphi_B), \qquad (2)$$

where Y is the photo yield which is a photocurrent per incident photon number. When $h\nu$ is close to the fundamental absorption edge, owing to the generation of electron-hole pairs, a large photocurrent flows, like a solar cell. Normally, a light from a monochrometer is used as a light source and irradiated to the entire metal/semiconductor interfaces. In this study, the wavelength was swept continuously from 310 to 1150 nm.

In the SIPM measurements, by focusing and scanning the beam over the interface, a two-dimensional image of Y can be obtained. After the Y mapping using the beams of two or more different wavelengths as well, the image of $q\varphi_B$ can be obtained according to Eq. (2). The green ($\lambda = 517$ nm, $h\nu = 2.40$ eV) and blue ($\lambda = 447$ nm, $h\nu = 2.77$ eV) lasers were used in the SIPM measurements. From the line scanning at the edge of the electrode, the beam spot diameter was estimated to be about 2 μm. Because the positional

resolution of the stage is as small as 0.1 μm, the spatial resolution of the SIPM measurements can be determined by the beam diameter.

4 Experimental results and discussion

4.1 Conventional dot Firstly, a sample without any process problem was measured as a conventional dot. Figure 2 shows (a) forward and (b) reverse *I–V* characteristics of the sample. In the as-deposited condition, the forward *I–V* curve is linear in a voltage range from 0.3 to 0.7 V. From the extrapolation of this region, $q\varphi_B$ was obtained to be 0.95 eV. In the reverse *I–V* characteristics, the current is virtually constant, as low as in a picoampere range down to −10 V. After annealing at 400 °C, the forward bias current decreased by about two orders of magnitude. As a result of that, $q\varphi_B$ increased by 0.19 eV. Other research organizations have also reported that after 400 °C annealing, $q\varphi_B$ increased in the *I–V* characteristics for Ni/n-GaN Schottky contacts [19, 20]. Recovery of the process induced damages during the electron beam deposition would be responsible for this increase.

Figure 3 shows PR spectra before and after annealing. In the as-deposited condition, when $h\nu$ is larger than 1.0 eV, a photocurrent was detected. As $h\nu$ increased, a square root of Y lineally increased up to 3.3 eV. It can be considered that the photocurrent is based on Eq. (2). Therefore, $q\varphi_B$ was obtained to be 1.10 eV. When $h\nu$ is larger than 3.3 eV, the photocurrent dramatically dropped, because of the fundamental absorption in the thick GaN substrate. After annealing, basically the same PR spectrum was obtained, but $q\varphi_B$ increased to 1.38 eV. This increase is consistent with the *I–V* results. Considering the SIPM measurements, our green and blue laser lines are in the linear region of the square-root-of-Y plot, so that, it is confirmed that the choice of laser lines is reasonable to obtain $q\varphi_B$.

Figure 4(a) shows microscope images of the dots before and after annealing. The surfaces of the dots are smooth

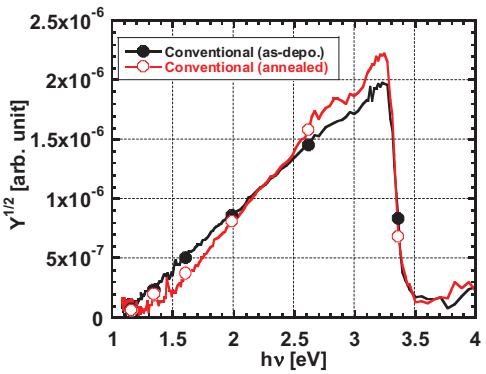

Figure 3 PR spectra of the conventional dot before and after annealing.

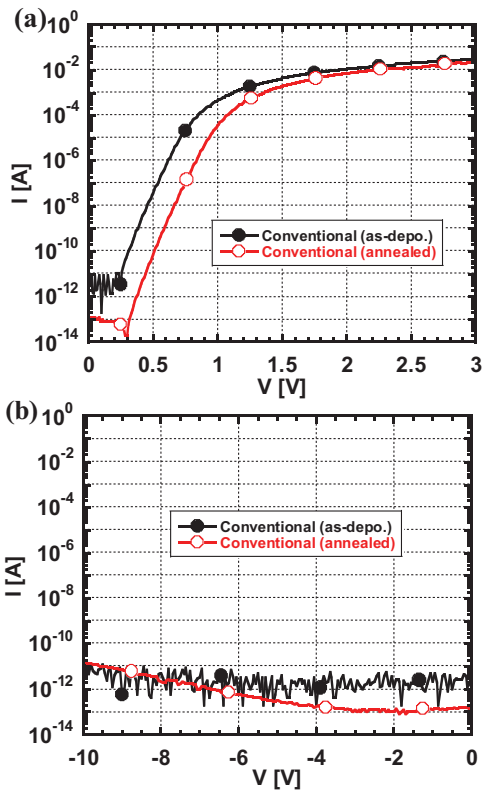

Figure 2 (a) Forward and (b) reverse *I–V* characteristics of the conventional dot before and after annealing.

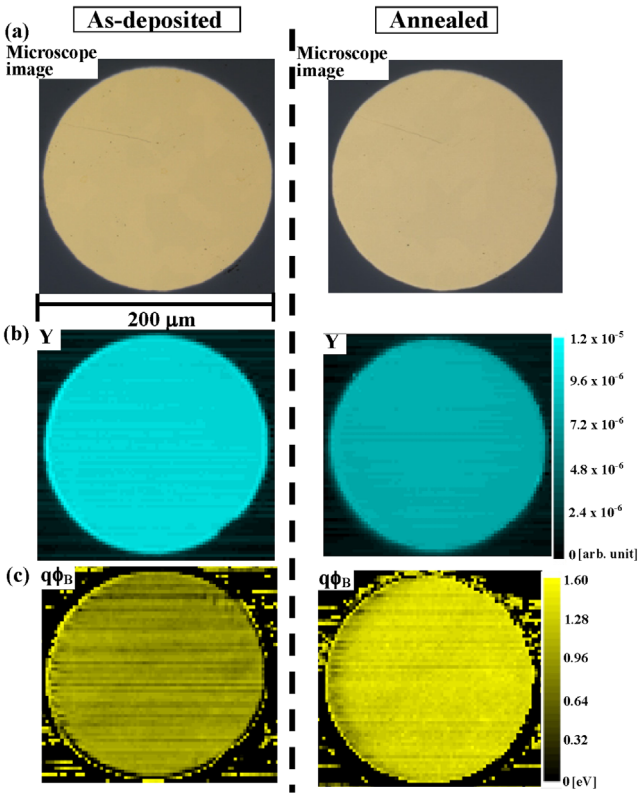

Figure 4 (a) Microscope, (b) *Y* and (c) $q\varphi_B$ images of the conventional dot before and after annealing.

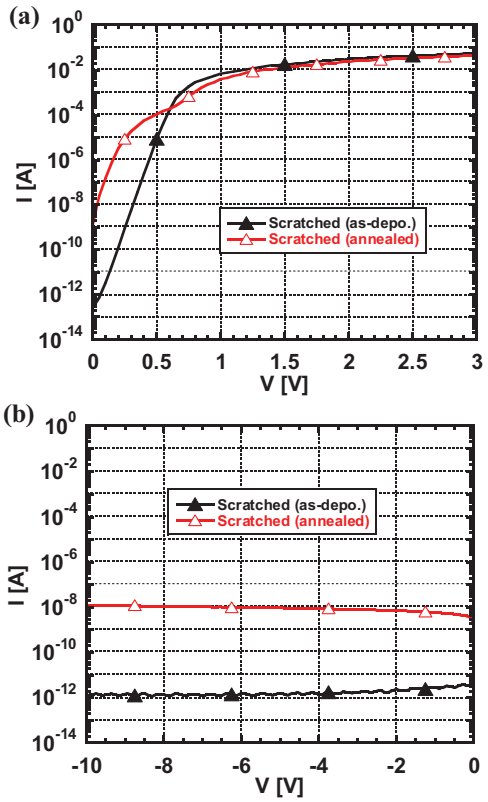

Figure 5 (a) Forward and (b) reverse *I*–*V* characteristics of the scratched dot before and after annealing.

even after annealing. Figure 4(b) shows *Y* images of the SIPM results with the blue laser. *Y* is uniform in a variation within 7% over the dots before and after annealing. Combining the *Y* images with the blue and green lasers, a $q\varphi_B$ image was obtained as shown in Fig. 4 (c). The $q\varphi_B$ value is also uniform and increased from 0.91 to 1.34 eV upon annealing, as well as the *I*–*V* results. These results tell us that conventional dots are uniform and free from thermal degradation at this annealing temperature.

4.2 Scratched dot Secondly, experimental results of the dot, in which the metal surface was scratched with small particles during the scribing and cutting processes before annealing are shown. Figure 5 shows the forward and reverse *I*–*V* characteristics of the scratched dot. In the as-deposited condition, the forward and reverse *I*–*V* curves are almost the same as those of the conventional dot. The $q\varphi_B$ value was obtained to be 0.95 eV. Even the metal surface was scratched, it is confirmed that there is no effect on the *I*–*V* characteristics. However, after annealing, the forward biased current increased by about 4 orders of magnitude and the apparent $q\varphi_B$ value decreased to 0.67 eV. The reverse biased current also increased by more than four orders of magnitude. On the other hand, the PR spectra are almost the same as those of the conventional dot before and after annealing (not shown here).

Figure 6(a) shows microscope images of the dot after annealing. Where the metal surface was deeply scratched, the metal layer was completely removed and the GaN surface was exposed (Fig. 7). In the *Y* images as shown in Fig. 6(b), no photocurrent was detected in these regions. Upon annealing, some regions with a more than four-times-larger *Y* appeared. This pattern can be also seen in the microscope image. These regions are located on the scratches. In order to investigate metal/GaN interface structure, the metal layer was etched away in an acid solution. Debris of the interfacial reaction can be seen and identified to the *Y* mapping pattern. A degradation model is

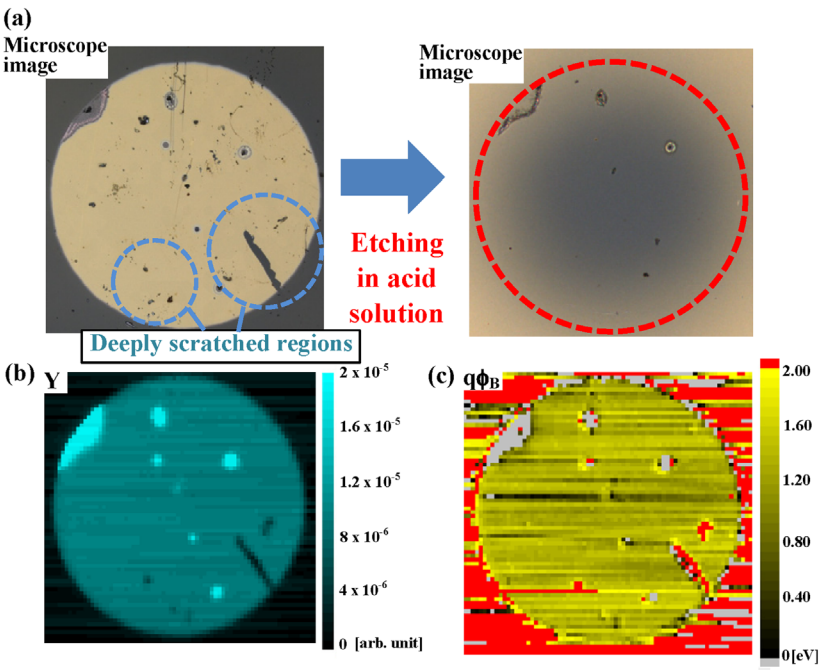

Figure 6 (a) Microscope, (b) *Y* and (c) $q\varphi_B$ images of the scratched dot.

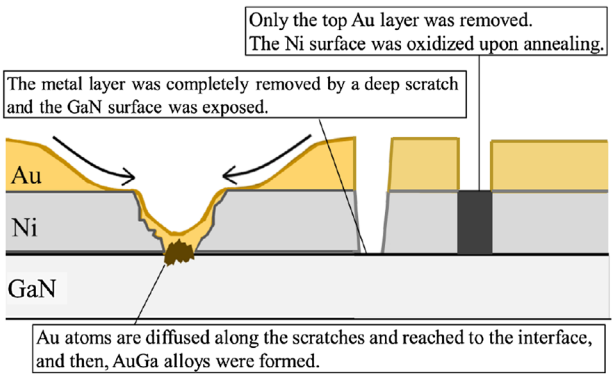

Figure 7 Surface structure of irregular dots after annealing.

proposed as shown in Fig. 7. There are same scratches, whose depth is within the Ni layer. It has been reported that in Au/Ni/p-GaN structure, upon annealing at 450 °C, Au atoms diffused through the Ni layer and reached to the GaN surface, and then a eutectic alloy of AuGa was confirmed by XRD measurements [21]. In a Au-Ga phase diagram, a eutectic temperature of γ-AuGa is 348.9 °C. Therefore, in our study, upon annealing at 400 °C, Au atoms are diffused along the scratches and reached to the interface, and then, AuGa alloys can be formed. Unfortunately, a reliable $q\varphi_B$ was not determined in these regions, because significant interfacial reaction occurred and the interface became ohmic-like. It is likely that this interfacial reaction also induced the leakage current in the *I*–*V* characteristics. It was confirmed that this method is useful to characterize partial thermal degradation as a map.

4.3 Dot with a partial removal of the Au layer The next irregular sample is a dot with a slight mechanical damage. Figure 8(a) shows the microscope images of the dot. In the as-deposited condition, the surface of a small portion of the dot is in silver color. In this region, the top Au layer was probably removed and the Ni surface was exposed (Fig. 7). Because the Au/Ni/GaN interface was preserved, *Y* and $q\varphi_B$ maps are uniform as shown in Fig. 8(b) and (c). After annealing, in the microscope image, the region became black. Even though the sample was annealed in the N_2 ambient, Ni surface may react with residual oxygen in a chamber. In the *Y* map, a 2.4-times-lager signal was obtained in this region. The $q\varphi_B$ value consistently decreased by 0.18 eV. There are two types of nickel oxides. NiO is reported to be a semiconductor with a band gap of between 3.6 and 4.0 eV in green [22, 23]. Ni_2O_3 is black, but its electrical characteristics have not been well understood. We are not sure the entire oxidation of the Ni layer all the way to the interface. Because the interfacial formation

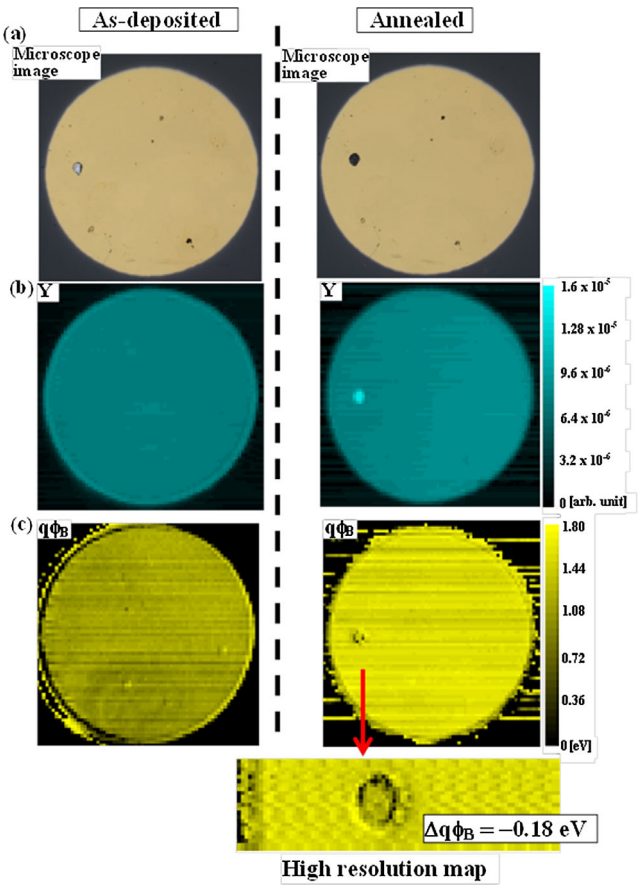

Figure 8 (a) Microscope, (b) *Y* and (c) $q\varphi_B$ images of the dot with a partial removal of the Au layer.

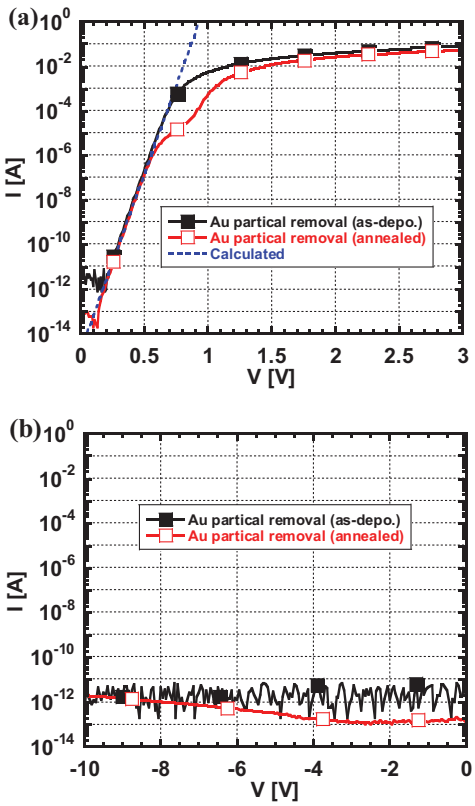

Figure 9 (a) Forward and (b) reverse *I*–*V* characteristics of the dot with a partial removal of the Au layer before and after annealing.

would be complicated, we considered that a NiO_x/GaN contact was newly formed.

Figure 9 shows forward and reverse *I–V* characteristics of this dot. In the as-deposited condition, the *I–V* curves are the same as those of the conventional dot. In the *I–V* characteristics of a conventional dot in Fig. 2(a), by annealing, the forward current decreased by about three orders of magnitude in the region where the current increased exponentially (from $V = 0.2$ to 0.7 V). The corresponding $q\varphi_B$ increased from 0.95 to 1.14 eV. The same behavior can be seen for Au/Ni/n-GaN region of the Au partial removal dot, resulting in the *I–V* curve after annealing between $V = 0.8$ and 1.0 V. On the other hand, upon annealing, the Ni exposed region was oxidized and $q\varphi_B$ became smaller by 0.18 eV than that of Au/Ni/n-GaN region. A current flow in the NiO_x/n-GaN region corresponds to the *I–V* curve between $V = 0.2$ and 0.7 V. The $q\varphi_B$ values of as-deposited Au/Ni/n-GaN and annealed NiO_x/n-GaN interfaces are almost the same, so that the forward and reverse *I–V* curves are also the same. Because the area and $q\varphi_B$ value of this region were determined by the SIPM measurements, a forward *I–V* curve can be calculated based on Eq. (1). Good agreement was obtained between measured and calculated curves in the low voltage region as shown in Fig. 9(a). These results tell us that this method is also useful to analyze a parallel contact of different interfacial phases in conjunction with the *I–V* characteristics.

4.4 Contaminated dot Finally, the sample with improper surface treatment was investigated. Figure 10(a) and (b) show conventional microscope and laser microscope images of the dot. A pattern of the contamination layer was seen in the marked region on the GaN bear surface. After annealing, this pattern appeared continuously on the dot. In the *Y* images, as shown in Fig. 10(c), the same pattern was observed. After annealing, the pattern almost disappeared. Because we have not conducted chemical analysis for the contamination layer, we are not sure for the reaction between Ni and the contamination layer. However, upon annealing, a pattern of the contamination layer clearly appeared on the dot in the laser microscope images [Fig. 10 (b)]. Therefore, it can be considered that the contamination layer desorbed from the interface. It has been reported that in Ni/native oxide/GaN structure, Ni diffused into the oxide layer by annealing at 400 °C for 10 min, and a pure Ni/GaN interface was formed [24]. In our study, it is likely that the same migration occurred, and a pattern of the contamination layer disappeared in the *Y* map. The same pattern also can be seen in the $q\varphi_B$ map as shown in Fig. 10(d). However, because the actual distribution of the photocurrent seems to

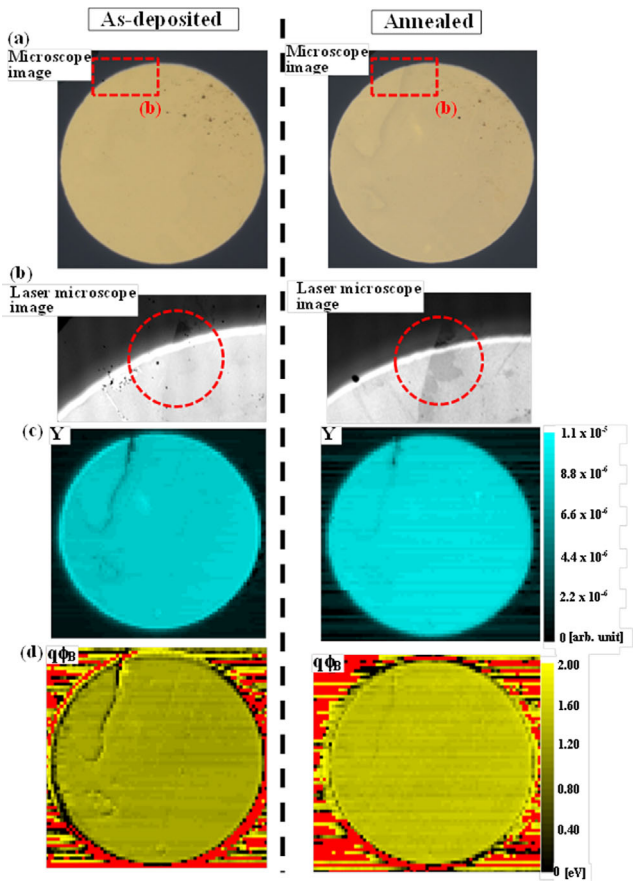

Figure 10 (a) Microscope, (b) laser microscope, (c) *Y* and (d) $q\varphi_B$ images of the contaminated dot.

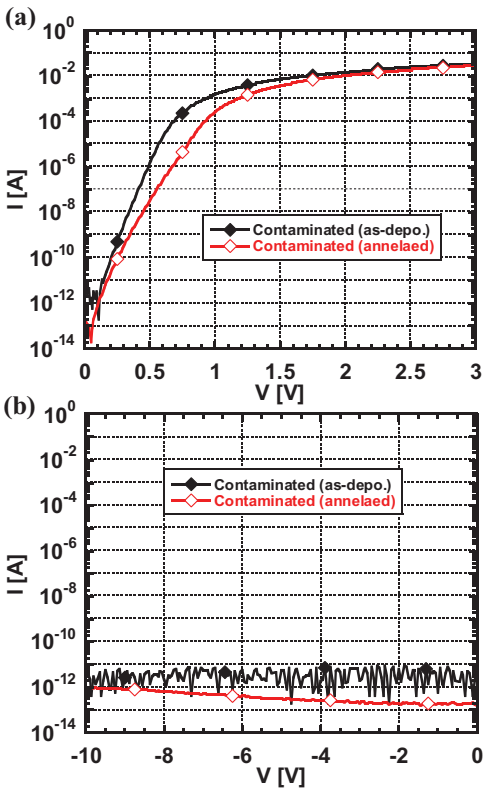

Figure 11 (a) Forward and (b) reverse *I–V* characteristics of the contaminated dot before and after annealing.

be very fine comparing with the laser beam diameter, the absolute value of $q\varphi_B$ is not reliable in the pattern.

Figure 11 shows forward and reverse *I–V* characteristics of the contaminated dot. In the as-deposited condition, the forward current of the contaminated dot is larger than that of the conventional dot by about one order of magnitude. A reliable $q\varphi_B$ value of the contaminated region could not been obtained in the SIPM measurements, but the *I–V* characteristics indicated that the Au/Ni/contamination layer/n-GaN interface has a lower $q\varphi_B$. After annealing, the *I–V* curve tends to be close to that of the conventional dot, but it was not completed in this annealing condition. It was found that this technique is very sensitive to the interfacial formation.

5 Conclusions We developed the SIPM measurement system to characterize wide bandgap semiconductor contacts, and the initial stage of thermal degradation of Au/Ni/n-GaN Schottky contacts were investigated. We found that, upon 400 °C annealing, a partial thermal degradation occurred from the scratch on the dot, where Au atoms diffused to the interface and reacted with GaN. When the top Au layer was partially missing, upon annealing, the Ni surface was oxidized and NiO_x/n-GaN with a small $q\varphi_B$ was formed. In addition, a thin contamination layer at the interface was clearly observed as a pattern. It was confirmed that this method is a powerful tool to map metal contacts for the investigations of partial thermal degradation, formation of parallel contacts, and inhomogeneity of surface chemistry.

Acknowledgements Apart of this work was supported by a Grant-in-Aid for Scientific Reserch C from the Ministry of Education, Culture, Sports, Science, and Technology.

References

[1] O. Toshihiro, M. Kanamura, Y. Kamada, K. Makiyama, Y. Inoue, N. Okamoto, K. Imanishi, K. Joshin, and T. Kikkawa, MRS Spring Meeting (2012).
[2] Z. Z. Bandic, P. M. Bridger, E. C. Piquette, T. C. McGill, R. P. Vaudo, V. M. Phanse, and J. M. Redwing, Appl. Phys. Lett. **74**, 1266 (1999).
[3] J. Joh and J. A. del Alamo, IEEE Trans. Electron Devices **58**, 132 (2011).
[4] M. Kanechika, M. Sugimoto, N. Soejima, H. Ueda, O. Ishiguro, M. Kodama, E. Hayashi, K. Itoh, T. Uesugi, and T. Kachi, Jpn. J. Appl. Phys. **46**, 503 (2007).
[5] Y. Saitoh, K. Sumiyoshi, M. Okada, T. Horii, T. Miyazaki, H. Shimoi, M. Ueno, K. Katayama, M. Kiyama, and T. Nakamura, Appl. Phys. Express **3**, 081001 (2010).
[6] Y. Hatakeyama, K. Nomoto, A. Terano, N. Kaneda, T. Tsuchiya, T. Mishima, and T. Nakamura, Jpn. J. Appl. Phys. **52**, 028007 (2013).
[7] P. Makaram, J. Joh, J. A. del Alamo, T. Palacios, and C. V. Thompson, Appl. Phys. Lett. **96**, 233509 (2010).
[8] J. A. del Alamo and J. Joh, Microelectron. Reliab. **49**, 1200 (2009).
[9] J. Joh, J. A. del Alamo, K. Langworthy, S. Xie, and T. Zheleva, Microelectron. Reliab. **51**, 201 (2011).
[10] L. Dobos, B. Pecz, L. Toth, J. Zs., Z. E. Horvath, A. Horvath, E. Toth, B. Horvath, Z. Beaumont, and Bougrioua, Appl. Surf. Sci. **253**, 655 (2006).
[11] L. D. Bell and R. P. Smith, J. Vac. Sci. Technol. B **16**, 4 (1998).
[12] T. Okumura and K. Shiojima, Jpn. J. Appl. Phys. **28**, 1108 (1989).
[13] K. Shiojima and T. Okumura, J. Cryst. Growth **103**, 234 (1989).
[14] K. Shiojima and T. Okumura, Proc. 29th Annual International Reliability Physics Symposium (IRPS), 234 (1991).
[15] H. S. Venugopalan, S. E. Mohney, B. P. Luther, S. D. Wolter, and J. M. Redwing, J. Appl. Phys. **82**, 650 (1997).
[16] G. L. Chen, F. C. Chang, K. C. Shen, J. Ou, W. H. Chen, M. C. Lee, and W. K. Chen, Appl. Phys. Lett. **80**, 595 (2002).
[17] S. M. Sze, Physics of Semiconductor Devices, 2nd ed. (Wiley, New York, 1981), pp. 245–311.
[18] R. H. Fowler, Phys. Rev. **38**, 45 (1931).
[19] J. D. Guo, F. M. Pan, M. S. Feng, R. J. Guo, P. F. Chou, and C. Y. Chang, J. Appl. Phys. **80**, 1623 (1996).
[20] Q. Z. Liu, L. S. Yu, F. Deng, S. S. Lau, and J. M. Redwing, J. Appl. Phys. **84**, 881 (1998).
[21] J. K. Sheu, Y. K. Su, G. C. Chi, P. L. Koh, M. J. Jou, C. M. Chang, C. C. Liu, and W. C. Hung, Appl. Phys. Lett. **74**, 2340 (1999).
[22] H. Yang, Q. Tao, X. Zhang, A. Tang, and J. Ouyang, J. Alloys Compd. **459**, 98 (2008).
[23] R. Newmant and R. M. Chrenko, Phys. Rev. **114**, 1507 (1959).
[24] H. Ishikawa, S. Kobayashi, S. Yamasaki, S. Nagai, J. Umezaki, M. Koike, and M. Murakami, J. Appl. Phys. **81**, 1315 (1997).